Front. Chem. China 2010, 5(1): 45–60
DOI 10.1007/s11458-009-0208-3

FEATURE ARTICLE

Organic photovoltaic materials and thin-film solar cells

Xin WANG[1], Di LIU[2] and Jiuyan LI (✉)[1]

1 State Key Laboratory of Fine Chemicals, Dalian University of Technology, Dalian 116012, China
2 Department of Chemistry, Dalian University of Technology, Dalian 116023, China

Organic photovoltaic materials are of interest for their future applications in solar cells. Compared to inorganic or dye-sensitized solar cells, organic photovoltaic (OPV) cells offer a huge potential for low-cost large-area solar cells because of their low material consumption per area and easy processing. In the last few years, there have seen an unprecedented growth of interest in OPVs with power conversion efficiency of over 5% attainable. However, OPV's performance is limited by the narrow light absorption, poor charge carries mobility, and low stability of organic materials, all of which confine its large-scale commercial applications. This review will develop a discussion on the OPV device configuration and operational mechanism after an introduction of the general features of OPV materials. Subsequently, the typical progresses in materials development and performance evolution in recent years will be summarized. The future challenges and prospects faced by organic photovoltaics will be discussed. Finally, the innovative strategy on research of molecular design and device optimization will be suggested with the aim for practical application.

Keywords solar cells, organic photovoltaics (OPV), organic thin film solar cells, power conversion efficiency

1 Introduction

The world's energy consumption is currently increasing with the subsequent consequences including environmental pollution and the greenhouse effect fron which people have suffered seriously. Therefore, it is one of the most important missions for human to develop novel clean and inexpensive energy sources. It is generally accepted that the solar energy is one of the most promising, available, renewable energy sources of all.

The solar cell is a photovoltaic (PV) device that converts sun light into electricity. Among all kinds of solar cells, inorganic semiconductors based solar cells have been developed very rapidly in the past decades and thus represent the most mature technology by taking up around 70% of photovoltaic markets nowadays. The silicon-based PVs have outstanding advantages in both efficiency and lifetime with power conversion efficiencies (PCE) in excess of 25% [1]. However, the high cost of raw materials and complicated processing techniques definitely limit their large-scale commercial developments. Accordingly, it is necessary to improve this technology and to decrease cost in a long run.

Therefore, a highly promising and cost-effective alternative for the photovoltaic energy sector is indispensable in the future. In this context, dye-sensitized solar cells (DSSC) have attracted considerable attention in recent years. At present, state-of-the-art DSSCs using ruthenium(II)-polypyridyl complexes as the active material have an overall power conversion efficiency approaching 11% under standard (Global Air Mass 1.5) illumination [2]. However, some expensive heavy metal sensitizing materials and unstable liquid electrolytes still confine the practical application of DSSCs.

In comparison with inorganic solar cells and DSSCs, organic photovoltaic cells (OPVs), also referred as organic thin film solar cells, have attracted much attention due to their potential advantages. From the first reports on molecular thin film devices more than 30 years ago, their power conversion efficiencies have increased considerably from 0.001% in 1975 [3] to 1% in 1986 [4] and more recently to 6.5% in 2007 [5]. Moreover, the PCE of 11% [6] might be attained in polymer/fullerene bulk heterojunction devices and 16% [7] in tandem

Received December 1, 2009; accepted December 21, 2009
E-mail: jiuyanli@dlut.edu.cn

devices according to simulation when the devices' level structure, the materials' optical band-gap and mobility are optimized simultaneously. Because the OPVs offer ease of fabrication and manipulation, flexibility, low weight and low cost, it should be possible and for the OPVs to become a true competitor to the silicon-based PV in the future. Furthermore, the huge development of research in the field of organic displays based on organic light emitting diodes (OLEDs) has contributed to the knowledge of the physics and chemistry of organic semiconductors. However, the OPVs is now only on the stage of theoretical research because of low PCEs limited by the low red absorption of organic materials, poor charge transport, and low stability. Therefore, in order to achieve the goals to solve the bottle-neck problems, they need to be improved not only in the aspects of the materials innovation and devices' structure optimization but also in theoretical research perfection.

In this review, first the general features of organic photovoltaic materials in comparison with inorganic semiconductors will be introduced. Subsequently the discussion will be focused on the OPV device structure and operational mechanism. The important advances in both OPV materials' development and performance evolution in recent years will be summarized. Furthermore, the future challenges and prospects faced by OPV materials and devices will be discussed. Finally, the innovative strategy on research of molecular design and device optimization will be suggested with the aim for practical application.

2 Features of OPV materials

Organic photovoltaic materials are conjugated solids with intense absorption in visible spectrum. Therefore both optical absorption and charge transport are dominated by partly delocalized π and π^* orbitals. Candidates for photovoltaic applications include crystalline or polycrystalline films of "small molecules", amorphous films of small molecules, films of conjugated polymers or oligomers, and combinations of any of these with either other organic solids or inorganic materials. Moreover, OPV materials have characters of intense and limited light absorption, and low stability that all limit the improvement of PCE. In detail, organic photovoltaic materials differ from inorganic semiconductors in the following important respects.

2.1 Light absorption

The optical excitations accessible to visible photons are usually π-π^* transitions. Most conjugated solids absorb in the blue or green; absorption in the red or infrared is more difficult to achieve. Therefore, the spectral range of optical absorption is relatively narrow less than 40% of the solar spectrum. That is one of reasons why power conversion efficiency of OPV is lower than that of inorganic semiconductors. Fortunately the absorption coefficients of organic materials are usually high ($\sim 10^5$ cm^{-1}) so that high optical densities can be achieved at peak wavelength and thus not too thick film of active layer (less than 100 nm thick) is required for OPV. In addition, most organic materials are sensitive to moisture and oxygen.

2.2 Exciton dissociation

Intermolecular van der Waals forces in organic solids are weak compared to covalent bonds in inorganic crystals. All electronic states are localized on single molecules and do not form bands. As a consequence, photogenerated excitations ('excitons') are strongly bound and do not spontaneously dissociate into separate charges. Upon absorption of a photon of sufficient energy by the organic semiconductor, an electron is promoted into the lowest unoccupied molecular orbital (LUMO), leaving behind a hole. However, due to electrostatic interactions, this electron-hole pair forms a tightly bound state named singlet exciton. The exact binding energy of this exciton is still under debate, but it is expected to be in a range of 200 to 500 meV [8,9]. Such binding energy is much higher than the thermal energy at room temperature (kT(300 K) = 26 meV [10,11]) and the binding energy of inorganic semiconductors (a few meV) as well. Consequently, optical absorption in organic materials does not directly lead to free electron and hole carriers that could readily generate an electrical current. Instead, the excitons must first dissociate in order to generate a current. The excitonic character of their optical properties is an inherent feature of organic semiconductors, and has impacted the design and geometry of organic photovoltaic devices for the past decades. For example, in the widely used poly (2-methoxy-5-(2'-ethyl-hexyloxy)-p-phenylene vinylene) (MEH-PPV), experiments revealed that only 10% of the excitons dissociate into free carriers in a pure layer [12], while the remaining excitons decay via radiative or nonradiative recombination pathways.

2.3 Charge mobility

In crystalline inorganic semiconductors, the three-dimensional character and rigidity of the lattice ensure wide valence and conduction bands and large charge carrier mobilities. However, the mobilities of organic semiconductors are several orders of magnitude less than those found in crystalline inorganic semiconductors [13]. Charge transport proceeds by hopping between localized states rather than transporting within a band, resulting in low mobilities. Even

the highest reported hole mobilities (μ_h) for organic semiconductors reach currently only about 15 $cm^2 \cdot V^{-1} \cdot s^{-1}$ for single crystals of small molecules [14] and 0.6 $cm^2 \cdot V^{-1} \cdot s^{-1}$ for liquid crystalline polymers [15] (Si: μ_h = 450 $cm^2 \cdot V^{-1} \cdot s^{-1}$). Highest electron mobilities (μ_e) for organic materials are typically lower, hovering around 0.1 $cm^2 \cdot V^{-1} \cdot s^{-1}$ [16,17] (Si: $\mu_e = 1400\ cm^2 \cdot V^{-1} \cdot s^{-1}$). The mobility values for most commonly amorphous organic materials used in organic solar cells are even several magnitudes lower. These low mobilities limit the feasible thickness of the organic layer in solar cells to a few hundred nanometres. Fortunately, organic semiconductors are very strong absorbers in the UV-Vis regime. Thus organic layers of only 100 nm thick are needed for effective absorption.

Consequently, these properties impose some constraints on organic photovoltaic devices. A strong driving force should be present to break up the photogenerated excitons. Low charge carrier mobility limits the useful thickness of devices. Limited light absorption across the solar spectrum limits the photocurrent. Photocurrent is sensitive to temperature through hopping transport.

3 Device configuration and mechanism

The process of conversion of light into electricity by an organic solar cell can be schematically described by the following steps (Figure 1): absorption of a photon leading to the formation of an excited state, i.e., the bound electron-hole pair (exciton) creation; exciton diffusion to a region where exciton dissociation, that is, charge separation occurs; and charge transport within the organic semiconductor to respective electrodes [18,19].

3.1 OPV device configuration

3.1.1 Homojunctions

The simplest organic solar cells can be made by sandwiching thin films of single-polar organic semiconductors between two electrodes with different work functions (typically indium tin oxide ITO and a low work function metal such as Al, Ca, Mg). The difference in work function provides an electric field that drives separated charge carriers towards the respective contacts. This design sets up a built-in electric field in the semiconductor [20]. When the organic semiconductor absorbs light, electrons are created on the lowest unoccupied molecular orbital (LUMO) level and holes are created on the highest occupied molecular orbital (HOMO) level. In principle, the built-in electric field can pull the photogenerated electrons to the low-work function electrode and holes to the high-work function electrode, thereby generating a current and voltage. In practice, however, these cells have very low power conversion efficiency ($< 0.1\%$) because the electric field is insufficient to separate the strongly bound excitons. Instead, the exciton diffuses within the organic layer until it reaches a contact where it may be broken up to supply separate charges or recombine. Since exciton diffusion lengths are as short as typically 1–10 nm, exciton diffusion limits charge carrier generation in such a device. Consequently, only a small proportion of excitons can reach electrodes and generate a current. Other loss factors are non-radiative recombination at the interfaces and non-geminate recombination at impurities or trapped charges.

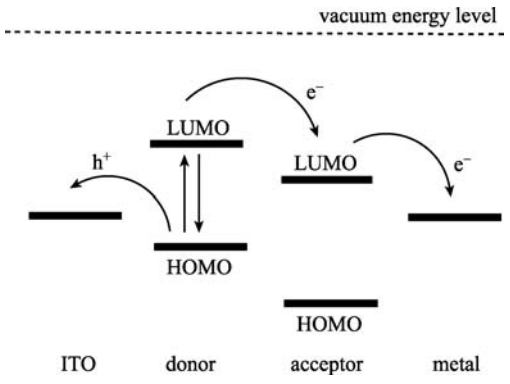

Figure 1 Operational principle of OPV.

3.1.2 Bilayer heterojunctions

The first bilayer device was designed by Tang [4] in 1986 and represented a major milestone in the field of organic photovoltaics (OPVs). It consists of a transparent electrode (typically a conducting oxide such as indium-tin oxide (ITO)), two organic light-absorbing layers, and a second electrode. Figure 2 illustrates the typical configuration of a bilayer heterojunction OPV device. The two organic layers are made of different organic semiconductors, one with an electron-donor character and the other with an electron-acceptor character. Electron-donor molecules (D) exhibit a low ionization potential, while electron-acceptor molecules (A) possess a high electron affinity. The D and A layers must provide efficient hole and electron transport, respectively. If both electron affinity and ionization potential are greater in one material (the electron acceptor) than the other (the electron donor), then the interfacial electric field drives charge separation. These local electric fields are strong and may break up photogenerated excitons, provided that the potential difference $\Delta\Phi$ between the ionization potential of the donor and the electron affinity of the acceptor is larger than the exciton binding energy [21]. However, this process, namely

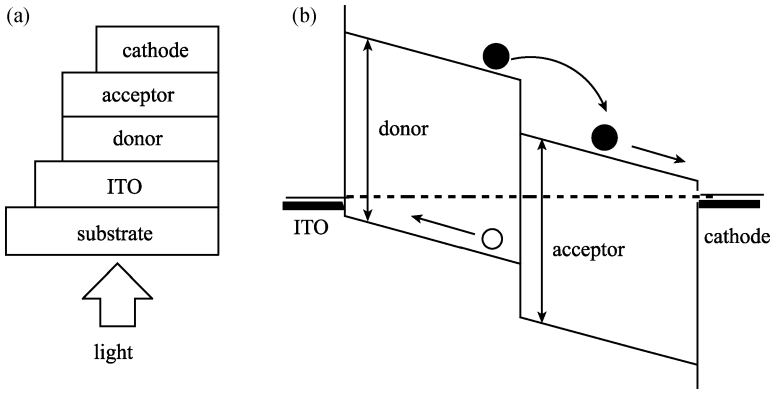

Figure 2 (a) Configuration and (b) energy level diagram of bilayer heterojunction OPV device.

photoinduced charge transfer, can lead to free charges only if the hole remains on the donor due to its higher HOMO level. In contrast, if the HOMO of the acceptor is higher, the exciton transfers itself completely to the material of lower-band gap accompanied by energy loss. In a bilayer heterojunction, the organic donor-acceptor interface separates excitons much more efficiently than the organic-metal interfaces in a single layer device.

3.1.3 Dispersed heterojunctions

A revolutionary development in organic photovoltaics came in the mid-1990s with the introduction of a dispersed heterojunction, where an electron accepting and an electron donating material are blended together (Figure 3). Since typical diffusion lengths are in the range of 10 nm, only a small portion of excitons can diffuse to D/A interface and then be dissociated. This limits efficient optical absorption. However, for most organic semiconductors the film thickness should be more than 100 nm in order to absorb most of the light. This problem can be overcome by blending the donor and the acceptor as a concept called dispersed (or bulk) heterojunction. Although bilayer heterojunctions are similar to dispersed heterojunctions in charge transfer through D/A interface effect, there are several main differences between them. (1) Charge separation in dispersed heterojunctions occur in the whole active layer, while charge carries in bilayer heterojuncions generate at the interface in a range of a few nanometers. As a consequence, the efficiency of excitons dissociation in dispersed heterojunctions is higher. If the length scale of the blend is similar to the exciton diffusion length, an exciton is likely to diffuse to an interface and break up wherever it is photogenerated in either material. (2) In the bilayer heterojunction, charge carriers transport towards respective electrodes in continuous pathways of the donor or acceptor. However, in the bulk heterojunction, both phases are intimately intermixed. Separated charges require percolated pathways for the hole and electron transporting phases to the contacts. In other words, the donor and acceptor phases have to form a nanoscale, bicontinuous, and interpenetrating network. Accordingly, the bilayer heterojunction has higher charge mobility than the bulk heterojunction. But one of

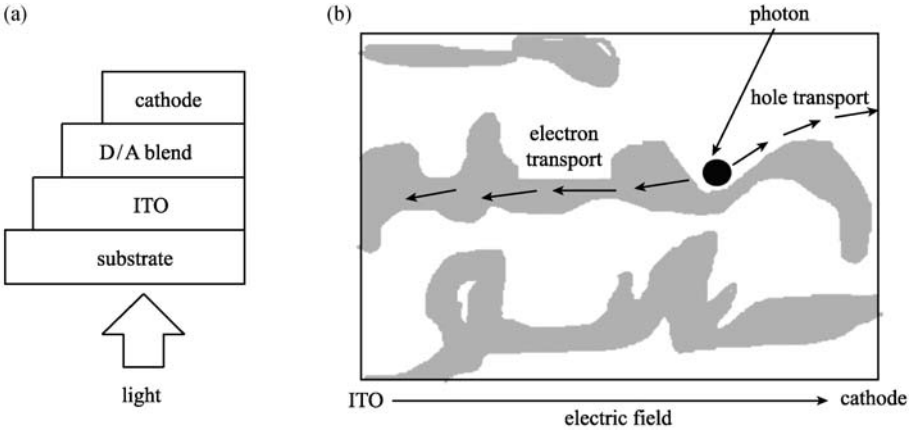

Figure 3 (a) Configuration of dispersed heterojunction OPV device. (b) The illustration of charge transportation pathways in the donor/acceptor blend film of such device.

the inherent problems with dispersed heterojunction is the solid-state miscibility due to large extended conjugated systems normally not miscible. Therefore, the bulk heterojunction devices are much more sensitive to the nanoscale morphology in the blend [22].

3.1.4 Donor-acceptor molecular heterojunctions

It is clear that the control of morphology in dispersed heterojunction devices is a critical point. The degree of phase separation and domain size depends on the choice of solvent, speed of evaporation, solubility, miscibility of the donor and acceptor, etc. One strategy towards increasing control is to covalently link donor and acceptor. This is a concept called donor-acceptor molecular heterojunction (as shown in Figure 4(a)). The driving force to separate photogenerated excitons is the chemical potential gradient between donors and acceptors, which not only accelerates charges separation but also drives charges carries transport to respective electrodes. According to the concept of donor-acceptor, the concept of "double cable" (Figure 4(b)) was introduced to monitor on the morphology at the molecular level. The chemical attachment of the electron acceptor moieties directly to the donor polymer backbone prevents the phase separation [23]. Electrons created by photoinduced electron transfer are transported by hopping between the pendent acceptor moieties, while the holes remain on the conjugated chain and transport along it. The efficiency of such devices is low probably due to fast recombination or inefficient interchain transport [24].

3.1.5 Tandem OPV

The "tandem cell" architecture [5] as shown in Figure 5 is a multilayer structure that offers a number of advantages. It is equivalent to two photovoltaic cells in series. Because the two cells are in series, the open-circuit voltage (V_{oc}) is increased to the sum of the V_{oc}'s of the individual cells. The use of two semiconductors with different band gaps enables the absorption over a broad range of photon energies within the solar emission spectrum. These two cells typically use a wide band-gap semiconductor for the first cell and a smaller band-gap semiconductor for the second. Because the electron-hole pairs generated by photons with energies greater than that of the energy gap rapidly relax to the respective band edges, the power-conversion efficiency of the two cells in series is inherently better than that of a single cell made from the smaller band-gap material. Therefore, the tandem cell architecture can possess a higher optical density over a wider fraction of the solar emission spectrum than that of a single cell without increasing the internal resistance. But the short-circuit current (I_{sc}) is lower than that of either single cell. Thus the overall power-conversion efficiency is mainly confined by photocurrent.

3.2 OPV mechanism

3.2.1 Optical absorption

There exist optical losses due to the mismatch between the solar spectrum and the band structure of the organic materials. Excess energy (E), which means the energy difference between the incident photon energy (E_A) and the energy gap (E_G) ($E = E_A - E_G$), is lost due to the thermalization of hot carriers. Alternatively, photons with too low energies ($E_A < E_G$) can not be absorbed. Hence the band gap E_G must be well adjusted. For example, the usage of materials with $E_G = 1.2$ eV instead of $E_G = 2.1$ eV allows a photon harvesting of 80% instead of 30% [25].

Furthermore, losses also happen due to an inappropriate sample thickness. If the sample is too thin, then part of the incident radiation will pass through the unabsorbed sample. As a consequence, there is no contribution to charge generation. However, if the sample is too thick, the exciton generation zone is too far from an interface where exciton dissociation occurs because the exciton diffuson lengths are less than 10 nm. Meanwhile, an unreasonable series resistance appears to decrease quantum efficiency.

Therefore, two compromises should possibly be made. First, the thickness of the organic sample must be sufficiently

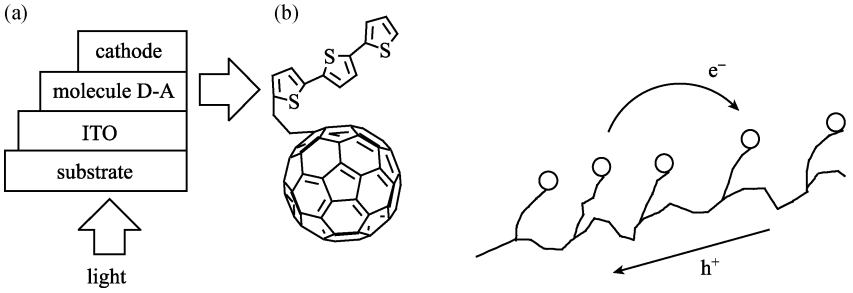

Figure 4 (a) Configuration of D-A molecular heterojunction OPV device and (b) the "double cable" D-A molecule.

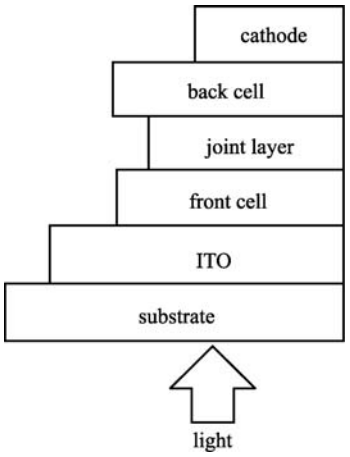

Figure 5 Typical structure of tandem OPV cell.

thick to absorb the radiation and sufficiently thin to allow charge generation in the vicinity of an interface (where exciton dissociation occurs), and to present a satisfactory series resistance. Second, the bandgap must be sufficiently small to absorb a maximum number of incident photons, and sufficiently large to limit sample aging induced by thermalization of hot electrons (which diminish with large band gaps).

3.2.2 Exciton dissociation

In single layer organic (polymer) photovoltaic cells, the internal field (built-in electric field) at the junction is evaluated at around $10^6\ \mathrm{V\cdot cm^{-1}}$, and the exciton dissociation yield is below 10% as indicated above. In order to reinforce the dissociation mechanism, a more efficient structure, built up of a donor–acceptor (D-A) heterojunction, is set up with organic- and polymer-based materials. The donor material has a low ionization potential (IP_D) from HOMO and the acceptor material has a high electron affinity (EA_A) from LUMO. If E_ex denotes the exciton energy in the donor material (energy of the electron-hole separation), the exciton binding energy in D materials is $E_{GD}-E_\mathrm{ex}$ (E_{GD} is the energy gap). After dissociation of the strongly bound exciton with a free electron in the acceptor material and a free hole in the donor, the corresponding state has an energy given by $IP_\mathrm{D}-EA_\mathrm{A}$. If $E_\mathrm{ex} > IP_\mathrm{D}-EA_\mathrm{A}$, the charge transfer reactions $\mathrm{D^*+A\rightarrow D^{+\cdot}+A^{-\cdot}}$ and $\mathrm{D+A^*\rightarrow D^{+\cdot}+A^{-\cdot}}$ will take place (see Figure 6(a)). Conversely, if $E_\mathrm{ex} < IP_\mathrm{D}-EA_\mathrm{A}$, such charge-transfer reactions are energetically unfavorable [25] (see Figure 6 (b)).

3.2.3 Charge transport

When holes and electrons are generated in donor and acceptor materials, they have to be transported through the bulk of the organic materials towards the electrodes (anode and cathode, respectively). For efficient photovoltaic devices, the created charges need to be transported to the appropriate electrodes within their lifetime. The charge carriers need a driving force to reach the electrodes [26]. This internal electrical field determines the maximum open circuit voltage (V_oc) and contributes to a field-induced drift of charge carriers. Also, the usage of asymmetrical contacts (one low work-function metal for the collection of electrons, and one high work-function metal for the collection of holes) is proposed to lead to an external field under short circuit condition within a metal-insulator-metal (MIM). Another driving force can be the concentration gradients of the respective charges. It leads to a diffusion current. During these bulk processes, trapping of carriers can occur. However, if carriers are trapped for a finite time (for example, in shallow traps), the mobility is affected. Carriers can finally be collected at electrodes without losses and the charge transport efficiency reaches up to unity. Conversely, if the carriers are trapped for an infinite time (by reacting with impurities, for example, oxygen in the bulk),

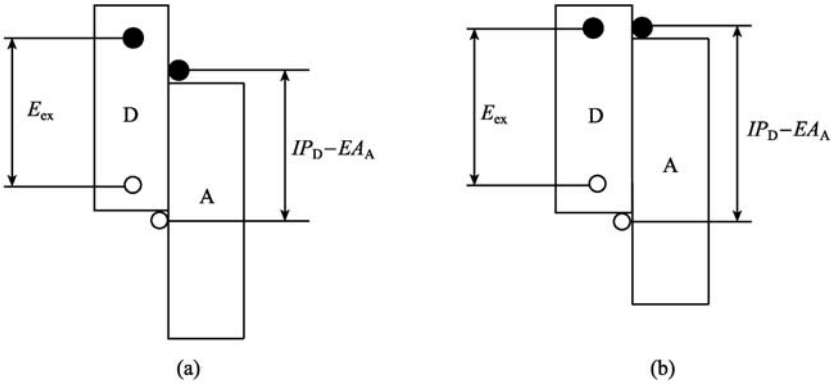

Figure 6 Schemetical illustration of exciton dissociation conditions: exciton dissociation is able to occur in case (a), but is energically unfavorable in case (b).

they are lost with respect to electrical current or bias voltage. Thus the charge carries' mobility not only depends on inherent characters, but also has correlation with charge traps effect.

4 Characterization of OPV performance

There are three critical parameters for solar cell efficiency: the open circuit voltage (V_{oc}), the short circuit current (I_{sc}), the fill factor (*FF*). Division of the maximum power (P_{max}) by the product of I_{sc} and V_{oc} yields the fill factor *FF*. The definition of these parameters is schematically illustrated in Figure 7.

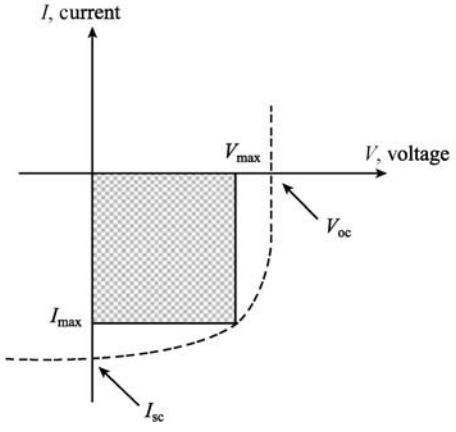

Figure 7 Typical *I-V* curve of OPV device under solar light irradiation.

4.1 Open circuit voltage (V_{oc})

In organic solar cells, V_{oc} is found to be linearly dependent on the energy difference between the HOMO of the donor and the LUMO of the acceptor [27,28]. Accordingly, those donor materials with low HOMO level and acceptors with high LUMO levels are usually applied in OPV devices in order to achieve high V_{oc} and efficiency. In addition, the V_{oc} is also found to be related to the interface contact between photovoltaic materials and electrodes [29]. Charge carrier losses at electrodes decrease the V_{oc} [30]. In order to achieve a better match between the energy levels of the anode and the HOMO of the hole conducting material, the commonly used ITO anode can be modified by plasma etching [31,32] or by coating with a higher work function organic hole transport layer [33,34]. The cathode is generally modified by deposition of a thin layer of LiF between the metal electrode and the organic semiconductor. This improves the charge injection and increases V_{oc} in organic solar cells [35]. Furthermore, the V_{oc} is also affected by the nanomorphology of the active layer [30].

4.2 Short circuit current (I_{sc})

In the ideal loss free contacts, I_{sc} is determined by the product of the photoinduced charge carrier density and the charge carrier mobility within the organic semiconductors [26].

$$I_{sc} = ne\mu E,$$

where n is the density of charge carriers, e is the elementary charge, μ is the mobility, and E is the electric field.

4.3 Fill factor (*FF*)

Fill factor is determined by charge carriers reaching the electrodes when the built-in field is lowered toward the open circuit voltage. In fact, there is a competition between charge carrier recombination and transport. Hence, the product of the lifetime μ times the mobility τ determines the distance d that charge carriers can drift under a certain electric field E: $d = \mu\tau E$. This product $\mu\tau$ has to be maximized [36]. Furthermore, the series resistances influence the filling factor considerably and hence should be minimized. Finite conductivity of the ITO substrate clearly limits the *FF* on large area solar cells [37].

4.4 Power conversion efficiency

There are three methods to express power conversion efficiency in solar cells: (1) external quantum efficiency (η_{EQE}), also called input photon conversion efficiency (η_{IPCE}); (2) internal quantum efficiency (η_{IQE}); (3) total power conversion efficiency (η).

The external quantum efficiency (η_{EQE}) is simply the number of electrons collected under short circuit conditions divided by the number of incident photons. η_{IPCE} is calculated using the following formula:

$$\eta_{EQE} = \eta_A \eta_{IQE} = \eta_A \eta_{ED} \eta_{ET} \eta_{CT} \eta_{CC},$$

where η_{IQE} is the internal quantum efficiency which denotes the number of electrons collected at the electrodes divided by absorbed photons in the device; η_A is the photon absorption efficiency; η_{ED} is the exciton diffusion efficiency; η_{ET} is the exciton dissociation efficiency; η_{CT} is the charge carries mobility; η_{CC} is the charge collection efficiency. η_{EQE} is also calculated using the following formula:

$$\eta_{EQE} = \frac{1240 \cdot I_{sc}}{\lambda \cdot P_{in}},$$

where λ (nm) is the incident photon wavelength, I_{sc} ($\mu A \cdot cm^{-2}$) is the photocurrent of the device, and P_{in} ($W \cdot m^{-2}$) is the incident power.

The photovoltaic power conversion efficiency of a solar cell is determined by the following formula:

$$\eta = \frac{P_m}{P_{\text{in}}} = \frac{V_{\text{oc}} I_{\text{sc}} FF}{P_{\text{in}}}.$$

The incident light power density P_{in} ($\text{W}\cdot\text{m}^{-2}$) is standardized at $1000\ \text{W}\cdot\text{m}^{-2}$ with a spectral intensity distribution matching that of the sun on the earth's surface at an incident angle of 48.2°.

5 Progress of OPV materials and devices

A major breakthrough happened in 1986 when Tang discovered that bringing a donor and an acceptor together in one cell could dramatically increase the PCE to 1%. This concept of heterojunction has ever since been widely exploited in a number of donor-acceptor cells, including dye/dye, polymer/dye, polymer/polymer and polymer/fullerene systems. Earlier problems in obtaining efficient charge carrier separation have been overcome. Different strategies have been used to gain better control over the morphology and to exploit new active materials with absorption further into the red to further improve efficiency. Now the power conversion efficiency of OPV has reached to 5%. And 6.5% has been reported recently.

5.1 Organic photovoltaic materials

5.1.1 Small molecules

Small molecules are known to have the highest charge carrier mobilities among overall organic semiconductors, and can be deposited to form thin films via vacuum thermal evaporation during which the gradient sublimation of low molecular weight molecules permits high levels of purification. Moreover, the synthesis of small molecules is usually simpler than that of polymeric semiconductors. Commonly, small molecular materials involved in OPVs include fullerenes and their derivatives, phthalocyanines, aromatic fused ring compounds, aromatic amines, and so on. The chemical structures of all the organic photovoltaic materials discussed in this review are shown in Figure 8.

(1) Fullerene C_{60} and its derivatives

The buckminsterfullerene C_{60} (as shown in Figure 8) is a good electron acceptor in OPVs with strong electron affinity and excellent electron transport nature, which can be electrochemically reduced up to 6 electrons [38]. For photoinduced electron-transfer reactions, it has been blended into electron-donating matrices with hole conducting materials of small molecules (such as phthalocyanine and thiophene oligomer) and polymers (such as polythiophene and polyphenylenevinylene). The application of simple C_{60} is limited because of its poor solubility in most common organic solvents. Accordingly a soluble derivative of C_{60}, PCBM (1-(3-methoxycarbonyl) propyl-1-phenyl[6,6]C_{61}) [39], has been invented by Wudl. PCBM is widely used in polymer/fullerene solar cells due to its good solubility. It would be safe to say that fullerene derivatives are currently the most successful type of electron acceptors in OPVs.

(2) Phthalocyanines

Phthalocyanine (Pc) is a planar molecule that contains four different indole units. Phthalocyanines include metal phthalocyanine (MPc) such as copper phthalocyanine (CuPc), zinc phthalocyanine (ZnPc) and tin (II) phtalocyanine (SnPc), nonmetal phthalocyanine dye (H2Pc) and subphthalocyanine (SubPc). Generally, MPc is usually donor material due to its strong light absorption at 700 nm and the character of *p*-type semiconductor. For the past 20 years, CuPc has been the donor of choice in most small molecule based solar cells due to its high stability, high mobility, and widespread availability [40]. SubPc's good photovoltaic performance has been indicated because of its unique structure and strong donor properties [41].

(3) Aromatic fused ring compounds

Aromatic fused ring compounds have large conjugated planar structure with strong semiconductor characteristics and tend to form orderly thin film. For example, a perylene derivative, 3,4,9,10-perylene tetracarboxylic bis-benzimidazole (PTCBI), is often used as acceptor materials due to its good photosensitivity and ease of crystallization in favor of electronic transmission. Pentacene is perhaps the most ubiquitous small-molecule organic semiconductors. It is frequently used as electron acceptor in OPVs due to the mobility rivaling that of amorphous Si [42] and reasonable air stability [43]. Graphene, the only two dimensional crystal of sp^2 hybridized carbon, has attracted much attention since it was experimentally demonstrated that the material is stable under ambient conditions [44]. The graphene layer displays high electron mobility, long phase coherence and elastic scattering lengths, and quantum confinement effects [45].

(4) Aromatic amines

Aromatic amines (such as TCVA and TPD in Figure 8) have high degree of non-coplanarity. They are usually used as donor materials in OPVs due to their strong electron donating nature.

5.1.2 Polymers

Due to good solubility and large π conjugated system, most polymers are electron-donors in photoinduced electron

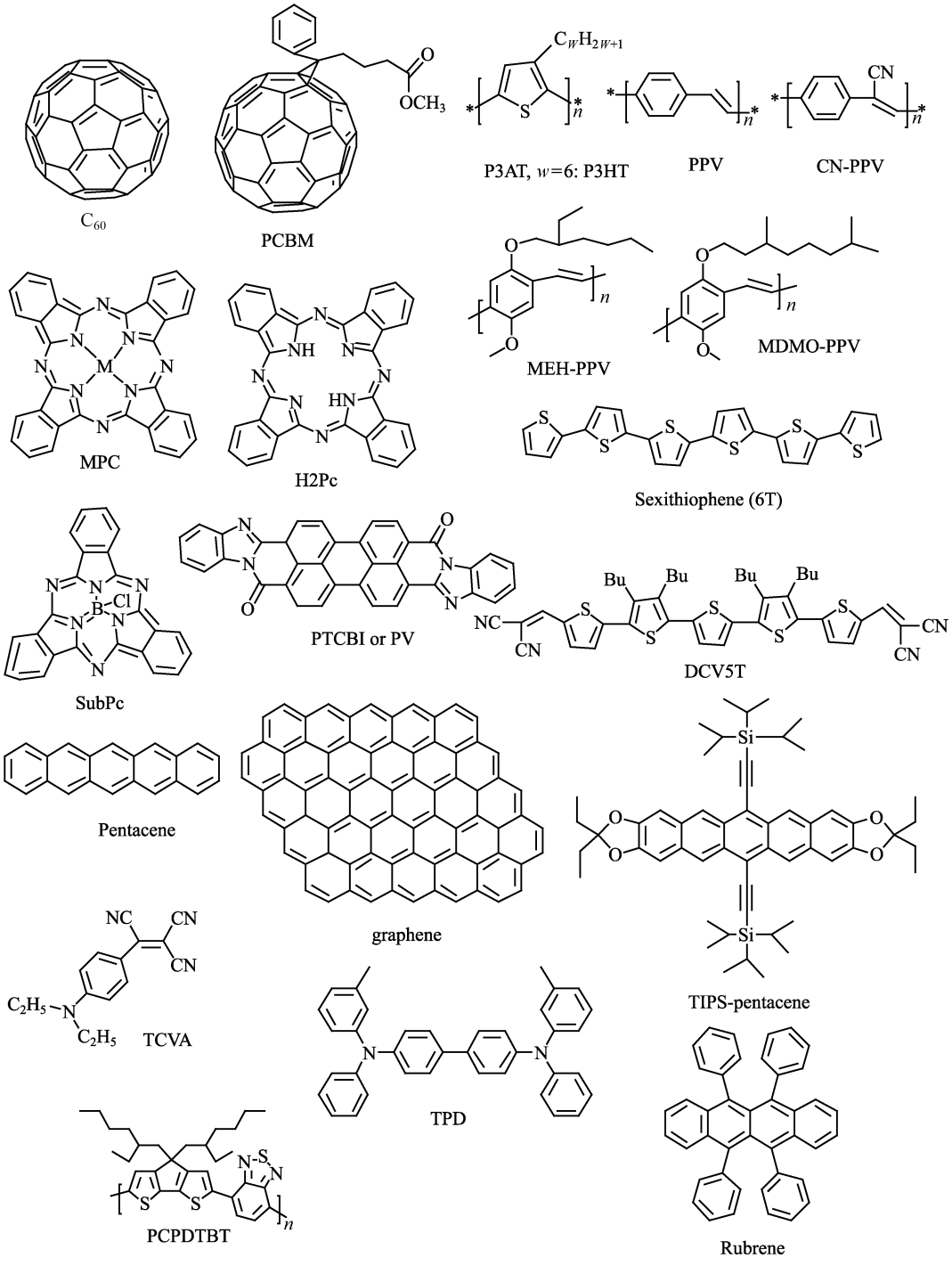

Figure 8 Chemical structures of the organic photovoltaic materials discussed in the present paper.

transfer process. They are superior to small molecules in that they are usually prepared by much simpler and cheaper spin-coating technique from a solvent in the process of OPV thin film production. The frequently used polymers in OPVs include polythiophene and polyphenylenevinylene (PPV).

(1) Polythiophenes

Thiophene is characterized by head-tail-connected orderly thin film leading to relatively high mobility. At present, the power conversion efficiency in the constitute of P3AT (poly (3-alkylthiophenes)) and C_{60} derivatives is the highest so far

(reaching to 5% among overall non-tendom OPVs). P3AT not only matches the solar spectrum, but also has good solubility and stability. Moreover, its morphology and crystallinity can be controlled and improved by heat treatment. Besides that, solvents also have impact on both absorption lengths and molecular aggregation phase [46]. In addition, micro-phase segregation of films can be achieved after the heat treatment, which is favorable of charges separation. Meanwhile, the crystallization formation of P3AT drives holes transport [47].

(2) Polyphenylenevinylene (PPV)

Polyphenylenevinylene (PPV) and its derivatives are widely studied in OPVs. As same as P3AT, charge transport can be improved through the heat treatment and the choice of solvents. PPVs are usually used as donor materials, and the best performance for PPVs are obtained from MEH-PPV [48] and MDMO-PPV [49] so far. However, one defect of PPV is its light oxidation with the consequences of destroying PPVs' backbone, leading to poor semiconductor performance and weaker light absorption. Meanwhile, with the appearance of deep level trap, charge carries mobility is reduced [50].

5.2 Development

5.2.1 Small molecule-based solar cells

The work of Tang in 1986 [4] is commonly cited as the groundbreaking discovery that sparked the current interest in the field. Using CuPc as the electron donor and PTCBI as the electron acceptor in a simple bilayer structure, a power conversion efficiency of 1% was reported. Later in 2005, a novel deposition method called vapour phase deposition (VPE) helped to further increase the efficiency for this system since a highly intermixed donor-acceptor interface could be obtained [51,52].

Although C_{60} does not show strong absorption properties in the visible region, its much larger exciton diffusion length and higher electron affinity (compared to PTCBI) is favorable to achieve higher efficiencies. Devices based on incorporating CuPc:C_{60} bulk heterojunctions reached power conversion efficiencies of up to 5% [53], which represents the highest efficiency for small molecule-based solar cells so far.

The drawback of using CuPc as an electron donor is that only relative small open circuit voltages can be reached with perylenes or fullerenes as acceptors. The reason is that a large portion of photon energy is wasted when the photogenerated electron on CuPc transfers to C_{60} or perylene. This problem can be solved by doping tris (8-hydroxyl-quinoline) aluminum (Alq_3) fluorescent dye into the acceptor or donor layers [54]. With Alq_3 doping, the increased photocurrent can be attributed to improved η_{ED} and broader spectral coverage. The increased V_{oc} is related to the increased energy difference between the LUMO of the acceptor layer and the HOMO of the donor layer. Alternatively the open circuit voltage could be increased by using other phthalocyanine derivatives with relarively low HOMO levels instead of CuPc as donor materials. Possible candicates include boron subphthalocyanine [55,56], aluminum phthalocyanine chloride (AlPcCl) [57] and tin (II) phtalocyanine (SnPc) [58,59].

Although the Pc:C_{60} system yielded high efficiency, it was still difficult to prepare bulk heterojunction OPV cells employing planar molecules due to their strong tendency to crystallize. A group of promising alternatives to phtalocyanines, i.e. oligothiophenes, were accordingly invented as donor materials. α,α-Bis(2,2-dicyanovinyl)-quinquethiophene (DCV5T) was reported by Schulze et al. [63] in 2006 as a good electron donor for OPVs since the HOMO level of DCV5T is sufficiently low (-5.6 eV), thus an open circuit voltages of 1V could be obtained. It was observed that suitable morphology could be obtained only for films deposited with the co-evaporation of excess C_{60}. It is likely that excess C_{60} prevents the crystallization of oligothiophene. Good PV performance in alpha-sexithiophen: (6T):fullerene bulk heterojunction PV cells was demonstrated for the first time [61]. Furthermore, a novel small molecule bulk heterojunction (BHJ) OPV cells consisting of oligothiophene 6T and a high fullerene (C_{70}) has been reported [62]. C_{70} is expected to possess a better electron transport and a higher photo-absorption property than C_{60} in the visible range. In addition to above donor materials, pentacene derivatives (such as 6,13-bis(triisopropylsilylethynyl) pentacene and TIPS-pentacene) [63] and rubrene semiconductor [64,65] were also brought into use in OPV devices recently. Lately, traditional colorants, such as squaraines, have been introduced. A series of squaraine dyes bearing an additional dicyanovinyl acceptor moiety at the central acceptor unit afford solution-processed BHJ solar cells with PCEs of up to 1.79%. More importantly, absorption in the highly desired near IR range and short-circuit current densities up to I_{sc}= 2.6 mA·cm^{-2} [66].

Since unsubstituted Pc are typically poorly soluble, enforcing application of vapor deposition techniques were invented for their incorporation into solar cells. Fischer introduced well soluble dendritic oligothiophenes to merge these systems with the soluble RuPc (phthalocyanines with four solubilizing peripheral tBu groups that incorporated ruthenium as metal center) complex with efficiencies of up to 1.6% achieved when blended together with a fullerene acceptor in solution-processed photovoltaic devices, providing by far the best phthalocyanine-based bulk heterojunction solar cells reported so far [67].

5.2.2 Polymer/polymer blend solar cells

In 1977, Chiang et al. [68] reported that doped polyacetylene could achieve metallic conductivity. This discovery initiated intense research on conjugated polymers. The first report on all polymer solar cells with moderate efficiencies dates back to 1995 [69]. MEH-PPV (poly(2-methoxy-5-(2'-ethyl-hexyloxy)-1,4-phenylene-vinylene)) was used as the electron donor and CN-PPV (cyano-para-phenylene vinylene) as the electron acceptor. External quantum efficiencies were still low (around 5%–6%). Using the copolymer M3EH-PPV as donor and CN-Ether-PPV as acceptor, Breeze et al. [70] demonstrated external quantum efficiencies of 24% (corresponding to 0.6% PCE) in 2000. Even higher efficiencies were achieved by the same authors in 2004 [71]. In that work, it was demonstrated for the first time that 1% PCE could be reached in a polymer/polymer blend device.

The highest PCE so far for solar cells composed of polymer blend was reported in 2005 by Kietzke et al. [72] using the same materials coupled with improved processing. An open circuit voltage of 1.36 V and a white light conversion efficiency of 1.7% were obtained. The fill factor reached 35%, indicating improved charge transport.

Polymer solar cells have much room for optimization. Both the *FF* and the quantum efficiency need to be doubled in order to reach a 6%–7% PCE. Recent experiments indicated that the device performance is currently limited largely by the low dissociation efficiency of the photogenerated excitons into free charge carriers. Even after dissociation, the electrons tend to localize near the heterointerface in the electron accepting polymers due to their amorphous nature. In order to proceed to higher efficiencies more crystalline electron acceptor polymers with larger electron mobilities are needed [73].

5.2.3 Polymer/small molecular dye solar cells

After the discovery in 1992 [74] that the transfer of photoexcited electrons from conjugated polymers to fullerenes is very efficient, polymer/C_{60} blend system has been a main research field in the past years.

Up to now, the record PCE of 5% was reported for polymer/dye solar cells in 2005, in which regioregular polythiophene derivative P3HT was used as electron donor and PCBM as acceptor. It was found that the degree of regioregularity, the polydispersities, and molecular weights of P3HT have an important influence on the device efficiency [75]. However, it seems that the reported efficiencies stagnated in 2005. Two main factors limit the device efficiency of the P3HT∶PCBM system to 5%.

First, the open circuit voltage reaches only 0.7 eV, which is quite small compared to the bandgap of P3HT (1.9 eV). A large amount of energy is lost when the photoexcited electron transfers from the LUMO of P3HT (around -3 eV) to the LUMO of PCBM (-3.8 eV). Recently it was pointed out that an efficiency of 10% may be reached with polymer/fullerene blends if the relative energy levels could be better aligned [76,77].

The second factor limiting the efficiency of P3HT∶PCBM cells is the absorption range of P3HT. P3HT absorbs visible light up to about 650 nm, meaning that most of the red portion of the visible spectrum and all infrared photons cannot be harvested. Efforts have been undertaken to increase the absorption range by synthesizing novel low-bandgap polymers. However, contrary to expectations, the low bandgap polymers synthesized with bandgaps as low as 1 eV usually did not result in devices with higher efficiency. One major problem with these low band-gap polymers was their low mobilities that limited the efficiency.

Recently, a series of new semiconducting polymers with alternating thieno[3,4-b]thiophene and benzodithiophene units have been synthesized and studied. The structural modifications optimized polymer's spectral coverage of absorption, their hole mobility, and miscibility with fulleride, and enhanced polymer solar cell performances. So far, a PCE of over 6% has been achieved in solar cells based on fluorinated polymers with alternating thieno[3,4-b]thiophene and benzodithiophene units/$PC_{61}BM$ composite films prepared from mixed solvents [78].

An organic photovoltaic device based on an acceptor of solution-processable functionalized graphene was designed in 2008. I_{sc} of 4.0 mA·cm^{-2}, V_{oc} of 0.72 V, and PCE of 1.1% were obtained for the device of ITO/poly(ethylene dioxythiophene) doped with polystyrene sulfonic acid (40 nm)/poly(3-hexylthiophene-1,3-diyl):grapheme (graphene 10 wt.%, 100 nm)/LiF (1nm)/Al (70 nm) after an annealing treatment under simulated AM 1.5G 100 mW illumination in air [79]. Because of the low price, ease of preparation, and inertness against ambient conditions, soluble graphene will be a promising candidate as acceptor materials in the photovoltaic applications.

Although P3HT is still dominating organic photovoltaic publication records, there are already several very promising alternative available polymers. These results have led to certified efficiencies beyond the best values reported for P3HT. Polymers with various band gaps produced certified efficiencies higher 5%. Novel material classes that are optimised for photovoltaic requirements will rapidly lead to efficiencies beyond 7%, and their combination in multi-junction devices will result in even higher efficiencies [80].

5.2.4 Tandem solar cells

Since a single organic material is unlikely to absorb efficiently from the blue to the infrared region, tandem structures were proposed in order to increase light absorption where different subcells absorb different wavelength regions. The difficulty in designing tandem solar cells is that the current of each subcell has to be matched. Recently in 2007, Kim et al. [5] reported tandem solar cells exceeding 6% conversion efficiency by using a TiO_x interlayer to separate the two subcells. (I_{sc}= 7.8 mA·cm^{-2}, V_{oc}= 1.24 V, FF = 0.67, η = 6.5%). It has been successfully demonstrated that the application of polymers: fullerene derivatives and bulk heterojunction tandem cells with each layer processed from solution. A transparent titanium oxide (TiO_x) layer separates and connects the front cell and the back cell. The TiO_x layer serves as an electron transport and collecting layer for the first cell and as a stable foundation that enables the fabrication of the second cell to complete the tandem cell architecture. Figure 9 shows an inverted structure with the low band-gap polymer-fullerene composite as the charge-separating layer in the front cell and the high band-gap polymer composite as that in the back cell.

Another simple tandem structure of OPVs cell for efficient light harvesting was demonstrated in 2008 [81]. In this device, a soluble fullerene derivative of PCBM is employed simultaneously to form a bilayer heterojunction PV subcell with the underlying CuPc, and a bulk heterojunction PV subcell with blended P3HT. In comparison with the conventional tandem structure, the omission of the semitransparent intercellular connection layer reduces the complexity of the device and the light loss. The enhanced short circuit current density (I_{sc}= 8.63 mA·cm^{-2}) and PCE (2.79%) of the tandem structure are nearly the sum of those of the stand-alone cells of CuPc/PCBM (I_{sc}= 2.09 mA·cm^{-2}, PCE = 0.43%) and P3HT:PCBM (I_{sc}= 6.87 mA·cm^{-2}, PCE = 2.50%).

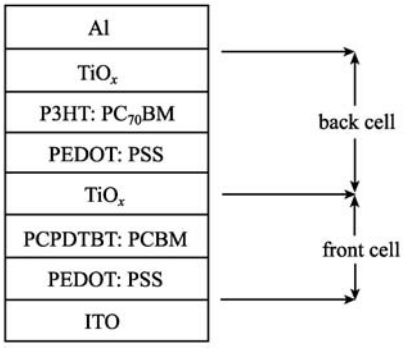

Figure 9 Structure of the reported tandem OPV cell with the highest efficiency of 6.5% so far.

6 Challenges and strategies

6.1 Competition and challenges

Inorganic solar cells are typically characterized by the *p-n* junction structure. In the vicinity of *p-n* junction, built-in electric field is formed from an abrupt *p-n* junction. The electron-hole pairs generated after the absorption of light diffuse to *p-n* junction interface, separate in the built-in electric field, and then move to the corresponding electrodes to form current. Based on the energy band character and narrow band gap nature of inorganic semiconductors, inorganic solar cells delivered the highest PCE of over 25% so far among all types of solar cells.

The single crystal silicon solar cells have been most maturely developed during the past decades and represented the highest PCE so far. However, the high production cost and complicated fabrication technique come to limit the large-scale practical application of the single crystal silicon solar cells. Alternatively, polycrystalline and amorphous silicon thin film solar cells have been developed. Polysilicon thin-film silicon solar cell has relatively lower cost than monocrystalline silicon solar cell and higher efficiency than amorphous silicon thin-film solar cell. Amorphous silicon thin film solar cell has advantages in low cost, light weight, and the great potential of mass production. But the limitation of photoelectric recession effect leading to low stability has a direct impact on practical application.

Besides Si, multicomponent materials like GaAs, CdS and copper-indium-selenium (referred as CIS), etc, are another important type of inorganic semiconductors which are frequently used in solar cells. The CdS polycrystalline solar cells are more efficient than amorphous silicon thin film solar cells, and have lower cost than single crystal silicon cells. They are also easy for mass production. However the highly toxic cadmium can cause serious environmental pollution. The III-V main group element compounds, like GaAs and copper-indium-selenium thin film solar cells, have relatively high PCE. Hence they are increasingly concerned. But the high expense of GaAs and rare source of indium, selenium elements are bound to limit the development of such kind of cells. In general, the high cost and serious corrosion of narrow band-gap semiconductors are the biggest problems encountered by inorganic solar cells.

The combination of organic dye sensitizer and wide band-gap inorganic semiconductor to generate DSSCs has ever been an innovative concept in the history of solar cells. Three active materials are used in DSSC: an organic dye as light absorber, a nanocrystalline metal oxide film (usually TiO_2) as electron transporter, and liquid or solid hole transporter. Dye

sensitization is a different strategy where a monolayer of a third material, usually an organic dye, is introduced between donor and acceptor to function as light absorber. Since light absorption and charge transport occur on different materials, the light absorber does not have to be a good bulk charge transporter. Therefore, they can be optimized individually to achieve the best combination to improve the possibility of high PCE. Large specific surface area and excellent electron transport ability of TiO_2 and good spectrum response of organic dyes make the photoelectricity conversion efficiency of DSSC up to around 10%. In comparison to inorganic solar cells, solid state DSSCs are most promising among organic-inorganic composite devices to date due to their low cost, low weight, and relatively easy production. Moreover, their good performance under diffuse light conditions is a feature they have in common with inorganic thin-film solar modules.

However, there still exist some problems concerning DSSC. N3 series dyes are currently recognized to deliver the best performance. But their complicated preparation process, high expense, and rare source make it necessary to explore novel dye systems. In addition, the highly saturated vapor pressure and poor stability in liquid electrolytes are austere challenges for large-scale applications. Furthermore, solid electrolytes with good stability have disadvantages in low ionic conductivity and poor interface contact with electrodes, leading to low PCE. Therefore, researchers are struggling to improve the conversion efficiency of solid electrolytes, or to use highly stable ionic liquid electrolytes as alternatives.

The need to develop inexpensive renewable energy sources stimulates scientific research for efficient, low-cost organic photovoltaic cells devices. The organic, polymer-based photovoltaic elements have shown us at least the potential of obtaining cheap and easy methods to produce energy from light. Organic semiconductors have several advantages including low-cost synthesis, and easy manufacture of thin film devices by vacuum evaporation/sublimation or solution cast or printing technologies. Besides, organic photovoltaic cells have potential advantages in large-area production, flexibility, environment-friendly and portability. All these merits make it possible to be applied in many power-supply systems such as watches, portable calculators, semi transparent chargers and toys.

However, the short circuit current, fill factor and power conversion efficiency of OPVs are all lower than those of other solar cells. The worse performance of OPVs is mainly caused by their narrower and weaker light absorption range, less efficient exciton dissociation, and weaker charge transportation.

6.2 Innovative strategies

Accordingly, most of current research is aimed to enhance light harvesting, improve charge carries mobility, increase device stability, and so on either by novel materials development or by processing technique optimization.

Effective strategies to enhance light harvesting include increasing absorption coefficiency, enlarging absorption range, and decreasing band gap of the active materials. Polymers are common donor materials in OPVs. However, most semiconducting polymers have band gaps higher than 2 eV (absorption edge at 620 nm), which definitely limits the possible harvesting of solar photons to about 30%. It was proven that the light absorption will be increased to near 80% if the polymer band gap is successfully decreased by intelligent molecular modification to below 1.1 eV, i.e. the absorption range is expanded into infrared region [82]. In addition, wide light absorption can be realized by addition of special materials with strong absorption character at a certain solar spectra range in the polymer films [82–84]. Until now, the development of BHJ solar cells has been essentially based on the use of soluble π-conjugated polymers as donor material. However, P3HT (as the standard donor material) and more general polymers have limited visible absorption because of their intrinsic electronic properties. Thus, various series of three-dimensional donors built by the attachment of different kinds of conjugated branches on a central node, including silicon, twisted bithiophene, triphenylamine, and borondipyrromethene (BODIPY), showed that the concept of a molecular donor with internal charge transfer at the same time leads to improved light-harvesting properties, red-shifted photoresponse, and a higher open-circuit voltage [85].

Charge transport in organic/polymeric materials is limited by the low intrinsic mobilities of organic solids and by the charge trapping effects of impurities and defects. Therefore, active materials with ordered phases and high mobility are expected to be developed. He et al. [46] studied bilayer OPVs consisting of different polythiophene, such as P3HT, P3OT, and P3DDT with different side chains, as electron-donor materials, and PCBM as electron acceptors. Due to the growth of side chains, head-tail connected regularity is affected by the consequences of low mobilities. Hence the PCE decreased from 1.54% to 0.59% along with the growth of side chains. Schilinsky et al. [86] investigated the effect of molecular weight of P3HT on solar cells performance. They found that with the increasing of molecule weight, absorption wavelengths of P3HT/PCBM(1∶1, wt) thin-film were red shifted and charges carries mobility increased. In addition, doping inorganic semiconductors possessing higher charge mobility into organic photovoltaic materials can improve the charge

mobility. For example, adding double-wall carbon nano-tubes in organic material increased the hole transport ability and consequently improved the OPV device performance [87]. Also an alternative type of polymer solar cell, based on a polymer/inorganic nanocrystal hybrid device structure, is appealing because of its relatively high electron mobility and the good physical and chemical stability of inorganic nanocrystals. Efficient charge transfer to nano-crystalline TiO_2 from various polymers such as PPV [88] and polythiophene [89] has been reported. Recent work presents polymer photovoltaic devices based on poly(3-hexylthiophene) (P3HT) and TiO_2 nanorod hybrid bulk heterojunctions. Interface modification of a TiO_2 nanorod surface is conducted to yield a very promising device performance of 2.20% [90]. TiO_2 is the most widely studied material in such structures, but the sensitization of other oxides (such as SnO_2) with polymers has been demonstrated [91] as well.

To control the morphology of active materials film, especially in dispersed heterojunction device, another essential way has been established to improve OPV performance. The main purpose to control morphology is to gain uniformly blended film of donor and acceptor materials to avoid aggregation and phase separation [92]. The control of morphology can be achieved from the following pathways: (1) by controlling processing conditions. For example, the choice of solvents, atmosphere, and substrate temperature were found to strongly influence the morphology of polymer blends [93,94]. (2) by self-organization. Self-assembly by ionically or electrostatically interacting monolayers has been used to construct structured heterojunctions [95,96]. Self-assembled monolayers can also be used to modify substrate surfaces in order to control the segregation of blend components [97]. (3) by synthesis of D-A copolymers. Positioning D and A groups on the same polymer backbone can ensure effective photoinduced D-A electron transfer under all conditions and can avoid the problems of phase segregation problems. D-A copolymers may be designed to absorb photons of longer wavelength than single polymers, and hence improve light harvesting, but charge extraction may be more difficult.

Finally, stability is a common problem with conjugated polymers and needs to be improved if satisfactory performance is desired for OPV. Several studies of performance and stability of organic solar cells have been carried out on polymer-fullerene devices. These devices exhibit improved performance with increasing temperature, which is an advantage over inorganic devices attributed to temperature dependent mobility [98]. However, the stability is still poor [99] and may be addressed by encapsulating cells.

7 Conclusion and outlook

OPV has undergone a major development during the last decades with the PCE increasing of several orders of magnitude. This progress makes the outlook for organic solar cells very bright. Efficiency greater than 5% has been achieved and many people are optimistic to the fact that 10% can be achieved by optimizing the processes described in this review. Higher efficiency requires improvements in absorption of red light, charge transport, and material stability. Recent researches have focused on the synthesis and testing of new photovoltaic materials in established device structures and on the development of new structures where morphology is controlled through self-assembly and processing conditions. In summary, organic photovoltaics provides an exciting playground at the frontiers of science, engineering, and technology. If organic photovoltaics holds its promise, it can soon become an ubiquitous, clean, and sustainable technology for portable power and potentially provide large-scale energy production for future generations.

Acknowledgements We gratefully acknowledge the National Natural Science Foundation of China (Grant Nos. 20704002, 20602004, and U0634003), the Program for Changjiang Scholars and Innovation Research Team in university (IRT0711), and the NKBRSF (2009CB220009) for financial support of this work.

Jiuyan LI is currently an associate professor and Ph.D. supervisor at the State Key Laboratory of Fine Chemicals, Dalian University of Technology. She gained support from the Program for New Century Excellent Talents of the Ministry of Education of China since 2008. Her current research is focused on the development of novel organic materials for applications in optoelectronic devices, such as OLEDs and solar cells.

References

1. Chung, B. C.; Virshup, G. F.; Hikido, S.; Kaminar, N. R., *Appl. Phys. Lett*. **1989**, *55*, 1741–1743
2. Gao, F.; Wang, Y.; Zhang, J.; Shi, D.; Wang, M.; Humphrybaker, R.; Wang, P.; Zakeeruddin, S. M.; et al., *Chem.Commun*. **2008**, *23*, 2635–2637
3. Tang, C. W.; Albrecht, A. C., *J. Chem. Phys*. **1975**, *62*, 2139–2149
4. Tang, C. W., *Appl. Phys. Lett*. **1986**, *48*, 183–185
5. Kim, J. Y.; Lee, K.; Coates, N. E.; Moses, D.; Nguyen, T. Q.; Dante, M.; Heeger, A. J., *Science* **2007**, *317*, 222–225
6. Koster, L. J. A.; Mihailetchi, V. D.; Blom, P. W. M., *Appl. Phys. Lett*. **2006**, *88*, 093511-1–093511-3
7. Rand, B. P.; Burk, D. P.; Forrest, S. R., *Phys. Rev. B* **2007**, 75, 115327-1–115327-11

8. Marks, R. N.; Halls, J. J. M.; Bradley, D. D. C.; Friend, R. H.; Holmes, A. B., *J. Phys*. **1994**, *6*, 1379–1394
9. Barth, S.; Bässler, H., *Phys. Rev. Lett*. **1997**, *79*, 4445–4448
10. Brédas, J. L.; Cornil, J.; Heeger, A. J., *Adv. Mater*. **1996**, *8*, 447–452
11. Alvarado, S. F.; Seidler, P. F.; Lidzey, D. G.; Bradley, D. D. C., *Phys. Rev. Lett*. **1998**, *81*, 1082–1085
12. Miranda, P. B.; Moses, D.; Heeger, A. J., *Phys. Rev. B* **2001**, *64*, 081201-1–081201-4
13. Sirringhaus, H., *Adv. Mater*. **2005**, *17*, 2411–2425
14. Sundar, V. C.; Zaumseil, J.; Podzorov, V.; Menard, E.; Willett, R. L.; Someya, T.; Gershenson, M. E.; Rogers, J. A., *Science* **2004**, *303*, 1644–1646
15. McCulloch, I.; Heeney, M.; Bailey, C.; Genevicius, K.; MacDonald, I.; Shkunov, M.; Sparrowe, D.; Tierney, S.; et al., *Nat. Mater*. **2006**, *5*, 328–333
16. Anthopoulos, T. D.; Singh, B.; Marjanovic, N.; Sariciftci, N. S.; Montaigne R. A.; Sitter, H.; Colle, M.; de Leeuw, D. M., *Appl. Phys. Lett*. **2006**, *89*, 213504-1–213504-3
17. Gundlach, D. J.; Pernstich, K. P.; Wilckens, G.; Gruter, M.; Haas, S.; Batlogg, B., *J. Appl. Phys*. **2005**, *98*, 064502-1–064502-8
18. Nunzi, J. M., *C. R. Physique*. **2002**, *3*, 523–542
19. Heremans, P.; Cheyns, D.; Rand, B. P., *Acc. Chem. Res*. **2009**, *42*, 1740–1747
20. McGehee, M. D.; Goh, C., *Phys. Sustain Energy* **2008**, *1044*, 322–330
21. Kietzke, T., *Adv. OptoElectron* **2007**, 40285-1–40285-15
22. Yang, F.; Shtein, M.; Forrest, S. R., *Nat. Mater*. **2005**, *4*, 37–41
23. Cravino, A.; Sariciftci, N. S., *Mater. Chem*. **2002**, *12*, 1931–1943
24. Cravino, A.; Sariciftci, N. S., *Nat. Mater*. **2003**, *2*, 360–361
25. Moliton1, A.; Nunzi, J. M., *Polym. Int*. **2006**, *55*, 583–600
26. Gnes, S.; Neugebauer, H.; Sariciftci, N. S., *Chem. Rev*. **2007**, *107*, 1324–1338
27. Brabec, C. J.; Cravino, A.; Meissner, D.; Sariciftci, N. S.; Fromherz, T.; Rispens, M. T.; Sanchez, L.; Hummelen, J. C., *Adv. Funct. Mater*. **2001**, *11*, 374–380
28. Scharber, M. C.; Műhlbacher, D.; Koppe, M.; Denk, P.; Waldauf, C.; Heeger, A. J.; Brabec, C. J., *Adv. Mater*. **2006**, *18*, 789–794
29. Hoppe, H.; Sariciftci, N. S., *J. Mater. Res*. **2004**, *19*, 1924–1945
30. Mallairas, G. G.; Salem, J. R.; Brock, P. J.; Scott, J. C., *J. Appl. Phys*. **1998**, *84*, 1583–1587
31. Wu, C. C.; Wu, C. I.; Sturm, J. C.; Kahn, A., *Appl. Phys. Lett*. **1997**, *70*, 1348–1350
32. Sugiyama, K.; Ishi, H.; Ouchi, Y.; Yukio; Seki, K., *J. Appl. Phys*. **2000**, *87*, 295–298
33. Scott, J. C.; Carter, S. A.; Korg, S; Angelopoulos, M., *Syn. Meth*. **1997**, *85*, 1197–1200
34. Brown, J. M.; Kim. J. S.; Friend, R. H.; Cacialli, F.; Daik, R.; Feast, W. J., *Appl. Phys. Lett*. **1999**, *75*, 1679–1681
35. Brabec, C. J.; Shaheen, S. E.; Winder, C.; Sariciftci, N. S.; Denk, P., *Appl. Phys. Lett*. **2002**, *80*, 1288–1290
36. Riedel, I.; Dyakonov, V., *Phys. Status Solidi A* **2004**, *201*, 1332–1341
37. Maennig, B.; Drechsel, J.; Gebeyehu, D.; Kozlowski, F.; Werner, A.; Li, F.; Grundmann, S.; Sonntag, S.; et al., *Appl. Phys. A* **2004**, *79*, 1–14
38. Allemond, P. M.; Koch, A.; Wudl, F.; Rubin, Y.; Diederich, F.; Alvarez, M. M.; Anz, S. J.; Whetten, R. L., *J. Am. Chem. Soc*. **1991**, *113*, 1050–1051
39. Wudl, F., *Acc. Chem. Res*. **1992**, *25*, 157–161
40. Peumans, P.; Yakimov, A. V.; Forrest, S. R., *J. Appl. Phys*. **2003**, *93*, 3693–3723
41. Gommans, H. H. P.; Cheyns, D.; Aernouts, T.; Girotto, C.; Poortmans, J.; Heremans, P., *Adv. Funct. Mater*. **2007**, *17*, 2653–2658
42. Dimitrakopoulos, C. D., *Adv. Mater*. **2002**, *14*, 99–117
43. Facchetti, A., *Mater. Today* **2007**, *10*, 28–37
44. Novoselov, K. S.; Geim, A. K.; Morozov, S. V.; Jiang, D.; Zhang, Y.; Dubonos, S. V.; Grigorieva, I. V.; *Firsov*, A. A., *Science* **2004**, *306*, 666–669
45. Berger, C.; Song, Z.; Li, X.; Wu, X. S.; Brown, N.; Naud, C.; Mayou, D.; Li, T., et al., *Science* **2006**, *312*, 1191–1196
46. He, J.; Su, L., *Chin. Polym. Bull*. **2007**, *4*, 53–65
47. Yang, X. N.; Loos, J.; Veenstra, S. C.; Verhees, W. J. H.; Wienk, M. M.; Kroon, J. M.; Michels, M. A. J.; Janssen, R. A. J., *Nano Lett*. **2005**, *5*, 579–583
48. Tan, Z. A.; Yang, C. H.; Zhou, E. J.; Wang, X.; Li, Y. F., *Appl. Phys. Lett*. **2007**, *91*, 023509-1–023509-3
49. Shaheen, S. E.; Brabec, C. J.; Sariciftci, N. S.; Padinger, F.; Fromherz, T.; Hummelen, J. C., *Appl. Phys. Lett*. **2001**, *78*, 841–843
50. Pacios, R.; Chatten, A. J.; Kawano, K.; Durrant, J. R.; Bradley, D. D. C.; Nelson, J., *Adv. Funct. Mater*. **2006**, *16*, 2117–2126
51. Yang, F.; Shtein, M.; Forrest, S. R., *J. Appl. Phys*. **2005**, *98*, 014906-1–014906-10
52. Yang, F.; Shtein, M.; Forrest, S. R., *Nat. Mater*. **2005**, *4*, 37–41
53. Xue, J. G; Uchida, S.; Rand, B. P.; Forrest, S. R., *Appl. Phys. Lett*. **2004**, *84*, 3013–3015
54. Kao, P. C.; Chu, S. Y.; Huang, H. H.; Tseng, Z. L.; Chen, Y. C., *Thin Solid Films* **2009**, *517*, 5301–5304
55. Mutolo, K. L.; Mayo, E. I.; Rand, B. P.; Forrest, S. R.; Thompson, M. E., *J. Am. Chem. Soc.* **2006**, *128*, 8108–8109
56. Gommans, H.; Verreet, B.; Rand, B. P.; Muller, R.; Poortmans, J.; Heremans, P.; Genoe, J., *Adv. Funct. Mater*. **2008**, *18*, 3686–3691
57. Kim, D. Y.; So, F.; Gao, Y. L., *Sol. Energy Mater. & Sol. Cells* **2009**, *93*, 1688–1691
58. Rand, B. P.; Xue, J. G.; Yang, F.; Forrest, S. R., *Appl. Phys. Lett*. **2005**, *87*, 233508-1–233508-3
59. Kim, D. Y.; Sarasqueta, G.; So, F., *Sol. Energy Mater. & Sol. Cells* **2009**, *93*, 1452–1456
60. Schulze, K.; Uhrich, C.; Schűppel, R.; Leo, K.; Pfeiffer, M.; Brier, E.; Reinold, E.; Baeuerle, P., *Adv. Mater*. **2006**, *18*, 2872–2875
61. Sakai, J.; Taima, T.; Saito, K., *Org. Electron*. **2008**, *9*, 582–590
62. Sakai, J.; Taima, T.; Yamanari, T.; Saito, K., *Sol. Energy Mater.*

& Sol. Cells **2009**, *93*, 1149–1153
63. Lane, P. A.; Palilis, L. C.; Kushto, G, P.; Kafafi, Z. H.; Purushothaman, B.; Anthony, J. E., *Org. Photovoltaics* **2008**, *7052*, 70521J-1–70521J-6
64. Taima. T.; Sakai, J.; Yamanari, T.; Saito, K., *Jpn. J. Appl. Phys*. **2006**, *45*, 995–997
65. Taima, T.; Sakai, J.; Yamanari, T.; Saito, K., *Sol. Energy Mater. & Sol. Cells* **2009**, *93*, 742–745
66. Mayerhőffer, U.; Deing, K.; Gruss, K.; Braunschweig, H.; Meerholz, K.; Wuerthner, F., *Angew. Chem. Int. Ed*. **2009**, *48*, 8776–8779
67. Fischer, M. K. R; Lopez-Duarte, I.; Wienk, M. M.; Martinez-Diaz, M. V.; Janssen, R. A. J.; Bauerle, P.; Torres, T., *J. Am. Chem. Soc*. **2009**, *131*, 8669–8676
68. Chiang, C. K.; Fincher, C. R.; Park, Y. W.; Heeger, A. J.; Shirakawa, H.; Louis, E. J.; Gau, S. C.; MacDiarmid, A. G., *Phys. Rev. Lett*. **1977**, *39*, 1098–1101
69. Yu, G.; Heeger, A. J., *J. Appl. Phys*. **1995**, *78*, 4510–4515
70. Breeze, A. J.; Schlesinger, Z.; Carter, S. A.; Hoerhold, H. H.; Tillmann, H.; Ginley, D. S.; Brock, P. J., *Org. Photovoltaics* **2001**, *4108*, 57–61
71. Breeze, A. J.; Schlesinger, Z.; Carter, S. A.; Tillmann, H.; Horhold, H. H., *Sol. Energy Mater. & Sol. Cells* **2004**, *83*, 263–271
72. Kietzke, T.; Hőrhold, H. H.; Neher, D., *Chem. Mater*. **2005**, *17*, 6532–6537
73. Yin, C. H; Kietzke, T.; Neher, D.; Horhold, H. H., *Appl. Phys. Lett*. **2007**, *90*, 092117-1–092117-3
74. Sariciftci, N. S.; Smilowitz, L.; Heeger, A. J.; Wudl, F., *Science* **1992**, *258*, 1474–1476
75. Hiorns, R. C.; de Bettignies, R.; Leroy, J.; Bailly, S.; Firon, M.; Sentein, C.; Khoukh, A.; Preud'homme, H.; et al., *Adv. Funct. Mater*. **2006**, *16*, 2263–2273
76. Koster, L. J. A.; Mihailetchi, V. D.; Blom, P. W. M., *Appl. Phys. Lett*. **2006**, *88*, 093511-1–093511-3
77. Scharber, M. C., *Adv. Mater*. **2006**, *18*, 789–794
78. Liang, Y. Y., Feng, D. Q.; Wu, Y.; Tsai, S. T.; Li, G.; Ray, C.; Yu, L. P., *J. Am. Chem. Soc*. **2009**, *131*, 7792–7799
79. Liu, Q.; Liu, Z. F.; Zhang, X. Y.; Zhang, N.; Yang, L. Y.; Yin, S. G.; Chen, Y. S., *Appl. Phys. Lett*. **2008**, *92*, 223303-1–223303-3
80. Dennler, G.; Scharber, M. C.; Brabec, C. J., *Adv. Mater*. **2009**, *21*, 1323–1338
81. Zhang, C. F.; Tong, S. W.; Jiang, C. Y.; Kang, E. T.; Chan, D. S. H.; Zhu, C. X., *Appl. Phys. Lett*. **2008**, *92*, 083310-1–083310-3
82. Koeppe, R.; Sariciftci, N. S.; Büchtemann, A., *Appl. Phys. Lett*. **2007**, *90*, 181126-1–181126-3
83. Chan, M. Y.; Lai, S. L.; Fung, M. K.; Lee, C. S.; Lee, S. T., *Appl. Phys. Lett*. **2007**, *90*, 023504-1–0235504-3
84. Wong, H. L.; Mak, C. S. K.; Chan. W. K.; Djurisic, A. B., *Appl. Phys. Lett*. **2007**, *90*, 081107-1–081107-3
85. Roncali, J., *Acc. Chem. Res*. **2009**, *42*, 1719–1730
86. Schilinsky, P.; Asawapirom, U.; Scherf, U.; Biele, M.; Brabec, C. J., *Chem. Mater*. **2005**, *17*, 2175–2180
87. Somani, P. R.; Somani, S. P.; Flahaut, E.; Umeno, M., *Nanotech*. **2007**, *18*, 185708-1–185708-5
88. Savenije, T. J.; Warman, J. M.; Goossens, A., *Chem. Phys. Lett*. **1998**, *287*, 148–153
89. Spiekermann, S.; Smestad, G.; Kowalik, J.; Tolbert, L. M.; Gratzel, M., *Syn. Meth*. **2001**, *121*, 1603–1604
90. Lin, Y. Y.; Chu, T. H.; Li, S. S.; Chuang, C. H.; Chang, C. H.; Su, W. F.; Chang, C. P.; Chu, M. W.; et al., *J. Am. Chem. Soc*. **2009**, *131*, 3644–3649
91. Anderson, N. A.; Hao, E.; Ai, X.; Hastings, G.; Lian, T. Q., *Physica E* **2002**, *14*, 215–218
92. Chen, L. M.; Hong, Z. R.; Li, G.; Yang, Y., *Adv. Mater*. **2009**, *21*, 1434–1449
93. Arias, A. C.; MacKenzie, J. D.; Stevenson, R.; Halls, J. J. M.; Inbasekaran, M.; Woo, E. P.; Richards, D.; Friend, R. H., *Macromol*. **2001**, *34*, 6005–6013
94. Halls, J. J. M.; Arias, A. C.; MacKenzie, J. D.; Wu, W. S.; Inbasekaran, M.; Woo, E. P.; Friend, R. H., *Adv. Mater*. **2000**, *12*, 498–502
95. Schroeder, R.; Heflin, J. R.; Wang, H.; Gibson, H. W.; Graupner, W., *Syn. Meth*. **2001**, *121*, 1521–1524
96. Baur, J. W.; Durstock, M. F.; Taylor, B. E.; Spry, R. J.; Reulbach, S.; Chiang, L. Y., *Syn. Met*. **2001**, *121*, 1547–1548
97. Arias, A. C.; Corcoran, N.; Banach, M.; Friend, R. H.; MacKenzie, J. D.; Huck, W. T. S., *Appl. Phys. Lett*. **2002**, *80*, 1695–1697
98. Katz, E. A.; Faiman, D.; Tuladhar, S. M.; Kroon, J. M.; Wienk, M. M.; Fromherz, T.; Padinger, F.; Brabec, C. J.; et al., *J. Appl. Phys*. **2001**, *90*, 5343–5350
99. Padinger, F.; Fromherz, T.; Denk, P.; Brabec, C. J.; Zettner, J.; Hierl, T.; Sariciftci, N. S., *Syn. Met*. **2001**, *121*, 1605–1606